RAPID COMMUNICATIONS

PHYSICAL REVIEW E VOLUME 47, NUMBER 4 APRIL 1993

Structure factor for phase ordering in nematic liquid crystals

A. J. Bray
Department of Theoretical Physics, The University, Manchester M13 9PL, United Kingdom

Sanjay Puri
Department of Physics, University of Toronto, Toronto, Ontario, Canada M5S 1A7
and School of Physical Sciences, Jawaharlal Nehru University, New Delhi 110067, India

R. E. Blundell
Department of Theoretical Physics, The University, Manchester M13 9PL, United Kingdom

A. M. Somoza
Department of Physics, University of Toronto, Toronto, Ontario, Canada M5S 1A7
and Instituto de Ciencia de Materiales, CSIC, Universidad Autonoma (C-XII), Madrid E-28049, Spain
(Received 11 January 1993)

We present an approximate analytical calculation of the time-dependent structure factor for the phase-ordering dynamics of nematic liquid crystals. The structure factor is found to exhibit a k^{-5} tail, due to the presence of $\frac{1}{2}$ integrally charged string defects. Our theoretical results are in good agreement with simulation data, and are consistent with recent experiments.

PACS number(s): 61.30.−v, 64.60.Cn, 64.60.My

There has been considerable recent interest in the phase-ordering dynamics of systems which are not described by a simple scalar order parameter [1–10]. In particular, it has been predicted [4,5] that for a vector order parameter with rotational symmetry [described by the O(n) model], with $n \leq d$ where d is the dimension of space, the structure factor should exhibit a power-law tail,

$$S(\mathbf{k},t) \sim L(t)^{-n} k^{-(d+n)} \tag{1}$$

for $kL(t) \gg 1$ (but $ka \ll 1$), where $L(t)$ is the characteristic length scale at time t after a quench into the ordered phase and a is a microscopic length scale. Equation (1) generalizes Porod's law [11] (which applies for the case $n=1$), and can be understood very simply in terms of the topological defects in the order-parameter field [4–6,10]. A high density of such defects is nucleated by the initial quench, with the density decreasing during the subsequent coarsening process.

Nematic liquid crystals provide an ideal experimental system with a nonscalar order parameter. The first experiments [7,8] have been interpreted as being consistent with Eq. (1), with $n=3$ (and $d=3$). Unfortunately, however, nematic liquid crystals do not possess a simple O(n) symmetry, so the conditions under which (1) were derived do not hold. Nevertheless, the interpretation of (1) in terms of defects leads, as we shall see, to a natural generalization to nematic liquid crystals. To simplify the discussion we will work within the familiar equal-constant approximation [12]. Then there are two symmetries to consider: a global symmetry under rotations of the director $\mathbf{n}$, and a local inversion symmetry under $\mathbf{n} \rightarrow -\mathbf{n}$. The latter is absent in the O(3) model. The presence of the inversion symmetry means that, in addition to the monopole defects of the O(3) model, the nematic liquid crystal also possesses stable $\frac{1}{2}$ string defects [13], in which the director rotates through π on encircling the string.

Consideration of the possible stable defects leads to a simple interpretation of (1) [10]. Extending the scaling hypothesis beyond the scalar fields for which it was originally proposed [14], we assume that the real-space equal-time pair correlation function has the scaling form $C(\mathbf{r},t)=f(r/L(t))$. Fourier-transforming this result gives the structure factor $S(\mathbf{k},t)=L(t)^d g(kL(t))$. For $kL(t) \gg 1$, the structure factor probes length scales much shorter than $L(t)$. In this regime, therefore, one expects $S(\mathbf{k},t)$ to be the sum of contributions from independent defects, i.e., linear in the defect density ρ_{def}. For n-component vector fields, $\rho_{\text{def}} \sim L(t)^{-n}$. Extracting this factor from the scaling form for $S(\mathbf{k},t)$ yields (1) immediately. In particular, (1) implies k^{-5} and k^{-6} tails in the O(2) and O(3) models in $d=3$ due to string and monopole defects, respectively. In fact, the form of the power-law decay (and even its amplitude) can be calculated directly from the field of a single defect [15]. For nematic liquid crystals, this implies contributions of order k^{-5} and k^{-6} from strings and monopoles, respectively. The experimental finding of a k^{-6} tail [7,8] seems to imply, therefore, that scattering from monopoles dominates the structure factor at large $kL(t)$. The theoretical approach described here, however, leads to a k^{-5} tail, appropriate to string defects, and close to a recent simulation result that gave a tail exponent of about 5.3 [9]. Below we will show that both experiments and simulations over a limited range of $kL(t)$ tend to overestimate this exponent, and that both are actually consistent with an asymptotic exponent of 5. But first we present our analytical approach.

The order parameter for a nematic liquid crystal is [12] a 3×3 traceless, symmetric tensor Q. Within the equal-

 ©1993 The American Physical Society

constant approximation, an appropriate Ginzburg-Landau-Wilson free-energy functional (in dimensionless variables) is

$$F[Q]=\int d^3x[\tfrac{1}{2}\mathrm{Tr}(\nabla Q)^2+V(Q)] , \quad (2)$$

$$V(Q)=-\tfrac{1}{2}\mathrm{Tr}Q^2-\tfrac{1}{3}\mathrm{Tr}Q^3+\tfrac{1}{4}(\mathrm{Tr}Q^2)^2 . \quad (3)$$

The values of the coefficients in $V(Q)$ have been chosen for later convenience; the sign of the $\mathrm{Tr}Q^2$ term indicates that the system is in its ordered phase; the sign of the $\mathrm{Tr}Q^3$ term implies prolate ordering, as is appropriate for nematic liquid crystals. We take the dynamics to be given by the time-dependent Ginzburg-Landau equation $\partial_t Q=-(\delta/\delta Q)(F[Q]-\lambda\,\mathrm{Tr}Q)$, where λ is a Lagrange multiplier included to maintain the constraint $\mathrm{Tr}Q=0$. Using (2) for $F[Q]$, and using the constraint to eliminate λ, we have the equation of motion

$$\partial_t Q=\nabla^2 Q+Q+\{Q^2-(I/3)\mathrm{Tr}Q^2\}-Q\,\mathrm{Tr}Q^2 , \quad (4)$$

where I is the unit tensor. The dynamics thus contains two features: a diffusive behavior, represented by the $\nabla^2 Q$ term in (4), and a relaxational behavior represented by the other terms, which drive the order parameter locally to one of the minima of the potential $V(Q)$. It is the nontrivial interaction between these features that makes (4) extremely difficult to solve.

The essence of the theoretical approach for a *vector* order parameter is an approximate decoupling of these two aspects of the dynamics [4]. For the O(n) model, described by a vector field $\boldsymbol{\phi}$, the potential $V(\boldsymbol{\phi})$ has (with $\boldsymbol{\phi}$ suitably scaled) a degenerate ground-state manifold $\boldsymbol{\phi}^2=1$. The approximate equations for the vector theory [4] amount to introducing a diffusion field $\boldsymbol{\phi}^{(0)}$, and imposing $\boldsymbol{\phi}=\boldsymbol{\phi}^{(0)}/|\boldsymbol{\phi}^{(0)}|$ at late times to ensure that $\boldsymbol{\phi}$ lies on the ground-state manifold. This approach captures the essential features of the dynamics of the defects (defined by the zeros of $\boldsymbol{\phi}^{(0)}$) seeded by the initial conditions. We extend this methodology to the case of a tensor field as follows. We start by introducing a diffusive tensor field $Q^{(0)}$ satisfying

$$\partial_t Q^{(0)}=\nabla^2 Q^{(0)} , \quad (5)$$

and define

$$Q=f(Q^{(0)}) , \quad (6)$$

with the (tensor) function $f(Q^{(0)})$ obtained from the stable fixed points of Eq. (4). Thus the function $f(Q^{(0)})$ gives the stable minimum of the potential $V(Q)$ to which Q would flow under the dynamics (5) for a spatially uniform initial condition $Q^{(0)}$. To find f we introduce the quantities $R=\mathrm{Tr}Q^2$, $S=\mathrm{Tr}Q^3$, and work in the basis in which Q is diagonal. From (4) (omitting the diffusive term), R, S and the three elements Q_i of the diagonal tensor Q satisfy the equations

$$\partial_t Q_i=Q_i(1-R)+Q_i^2-R/3 , \quad (7)$$

$$\partial_t R=2R(1-R)+2S , \quad (8)$$

$$\partial_t S=3S(1-R)+R^2/2 . \quad (9)$$

Setting the left-hand sides to zero to find fixed points, and using (8) to eliminate S from (9), gives $R^*=0$, $\frac{2}{3}$, or $\frac{3}{2}$. The fixed point $R^*=0$ corresponds to $Q=0$, a local maximum of $V(Q)$. For $R^*=\frac{2}{3}$, (7) gives the fixed-point values Q_i^* as $-\frac{2}{3}$ and $\frac{1}{3}$. Imposing the traceless condition gives three diagonal fixed-point tensors Q whose (diagonal) elements (Q_1^*,Q_2^*,Q_3^*) are $(-\frac{2}{3},\frac{1}{3},\frac{1}{3})$ plus permutations. These correspond to oblate ordering (largest eigenvalue negative), and a stability analysis shows that these fixed points are *saddle points* of $V(Q)$. Finally for $R^*=\frac{3}{2}$, we find $Q_i^*=1$ or $-\frac{1}{2}$, giving fixed points $(1,-\frac{1}{2},-\frac{1}{2})$ plus permutations. These fixed points, which correspond to the desired prolate ordering (largest eigenvalue positive), are the required *global minima* of $V(Q)$.

Determining the function $f(Q^{(0)})$ amounts to finding the basins of attraction of the three stable fixed points. The complete set of fixed points, and their stabilities, are shown schematically in Fig. 1. From the symmetry of the figure it is clear that, if $Q^{(0)}$ is the diagonal matrix (Q_1,Q_2,Q_3), then the stable attractor for the initial condition $Q^{(0)}$ is the fixed point $(1,-\frac{1}{2},-\frac{1}{2})$ if Q_1 is the *largest* of the Q_i, and so on. Clearly for a general (not necessarily diagonal) tensor $Q^{(0)}$, the stable attractor has elements

$$Q_{ab}=f_{ab}(Q^{(0)})=\tfrac{3}{2}(n_a n_b-\tfrac{1}{3}\delta_{ab}) , \quad (10)$$

where the local director $\mathbf{n}$ is simply the eigenvector of $Q^{(0)}$ with largest eigenvalue. Representing space-time points $(\mathbf{r}_1,t)$, $(\mathbf{r}_2,t)$ by "1" and "2" respectively, with $r=|\mathbf{r}_1-\mathbf{r}_2|$, the two-point correlation function is given by

$$C(12)=\tfrac{2}{3}\langle \mathrm{Tr}\{f(Q^{(0)}(1))f(Q^{(0)}(2))\}\rangle , \quad (11)$$

where the factor $\frac{2}{3}$ normalizes the correlation function to unity at short distance, and the average is over the joint probability distribution for $Q^{(0)}(1)$ and $Q^{(0)}(2)$. The latter is readily calculated from (5). Taking the initial distribution of $Q^{(0)}$ to be Gaussian, it stays Gaussian at all times [because (5) is linear], and the required joint distribution is

$$P(Q^{(0)}(1),Q^{(0)}(2))=N\exp\left[-\frac{1}{1-\gamma^2}[\tfrac{1}{2}\mathrm{Tr}\{Q^{(0)}(1)^2+Q^{(0)}(2)^2\}-\gamma\,\mathrm{Tr}\{Q^{(0)}(1)Q^{(0)}(2)\}]\right] , \quad (12)$$

where $N=\frac{3}{4}[\pi^2(1-\gamma^2)]^{-5/2}$ is a normalization constant, and γ $[=\gamma(12)]$ is the normalized correlator of $Q^{(0)}$:

$$\gamma=\frac{\langle \mathrm{Tr}\{Q^{(0)}(1)Q^{(0)}(2)\}\rangle}{\langle \mathrm{Tr}Q^{(0)}(1)^2\rangle^{1/2}\langle \mathrm{Tr}Q^{(0)}(2)^2\rangle^{1/2}}$$
$$=\exp(-r^2/8t) , \quad (13)$$

and the final result follows trivially from (5).

We compute the average required in (11) by Monte Carlo methods [16]. Each $Q^{(0)}(i)$ $(i=1,2)$ involves *five* independent matrix elements. A convenient way to parametrize the matrix is to write the diagonal elements as $Q_{11}^{(0)}=\sqrt{2/3}x$, $Q_{22}^{(0)}=-x/\sqrt{6}+y/\sqrt{2}$, and

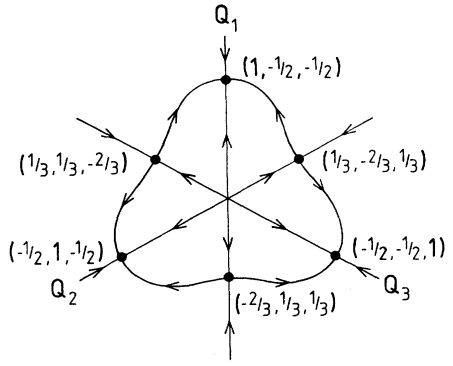

FIG. 1. Flow diagram (schematic) showing the basins of attraction of the three minima of the potential $V(Q)$ [Eq. (3)], namely $(1,-\frac{1}{2},-\frac{1}{2})$ and permutations. The coordinates of a point are obtained by dropping perpendiculars to each of the axes: all points in the plane satisfy $Q_1+Q_2+Q_3=0$.

$Q_{33}^{(0)}=-x/\sqrt{6}-y/\sqrt{2}$, in which the traceless condition is explicitly satisfied, and the off-diagonal elements as $Q_{ij}^{(0)}=z_{ij}/\sqrt{2}$ $(i<j)$, with $Q_{ji}^{(0)}=Q_{ij}^{(0)}$. At a given space point, x, y, z_{12}, z_{13}, and z_{23} are five independent, Gaussian random variables with zero mean and unit variance. However, a given variable (e.g., x) is spatially correlated with itself (but not with the other four variables), with correlator $\langle x(1)x(2)\rangle=\gamma$, given by (13). It is easy to verify that these rules are equivalent to the probability distribution (12).

To evaluate $C(12)$, a large number (at least 10^5) of pairs of Gaussian random matrices were generated, as described above, for each value of γ. For each matrix in a given pair, the eigenvector $\mathbf{n}$ corresponding to the largest eigenvalue was determined, and the corresponding tensor computed from (10). Finally, the average (11) was calculated over all pairs with a given γ. The results for $C(12)=f(x)$, plotted against the scaling variable $x=r/\sqrt{8t}$, are presented in Fig. 2. Also shown in Fig. 2 are the simulation data of Ref. [9]. The data have been rescaled, with $L(t)$ chosen to give the best fit to the theoretical curve at each time t [17]. The resulting fit is extremely good.

We have previously noted [9] that the equivalent theory for the O(2) model [4] also fits our real-space data well. The best fit is included in Fig. 2. Remarkably, it fits the data as well as Eq. (11). In fact, the simulation data for the O(2) model [2,18] and nematic liquid crystal [9] are virtually indistinguishable.

The main interest in the scaling function $f(x)$ is the short-distance behavior $(x\ll 1)$, since this determines the behavior of the structure factor for $kL(t)\gg 1$ [4,15]. A number of points in this range were determined with high precision, and the small-x behavior determined. A plot of $[1-f(x)]/x^2$ against $\ln x$ is linear at small x (see inset, Fig. 2), implying the small-x dependence

$$f(x)=1+ax^2\ln x-bx^2+\cdots, \tag{14}$$

where $a\simeq 1.11$, $b\simeq 0.65$. The presence of the $x^2\ln x$ term as the leading short-distance singularity in $f(x)$ implies a k^{-5} tail in its Fourier transform, the structure factor [4].

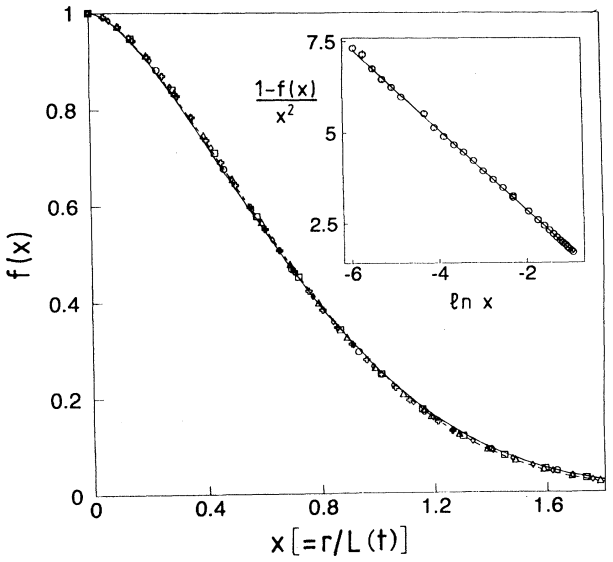

FIG. 2. Real-space scaling function $f(x)$, defined by $C(\mathbf{r},t)=f(r/L(t))$. Continuous curve: theoretical prediction (11), with $L(t)=\sqrt{8t}$. The inset shows that the small-x behavior of the theory is described by Eq. (14). Data points: simulation data from Ref. [9], with $L(t)$ fixed from the best fit to the theory; broken curve: best fit of the O(2) theory (Ref. [4]) to the data.

We looked for an x^3 term as the next leading term in (14), signaling a monopole contribution (and giving an additional k^{-6} term in the structure factor) but found no evidence for one: The next term in (14) seems to be $O(x^4)$ or, more likely, $O(x^4\ln x)$. We conclude that, within the

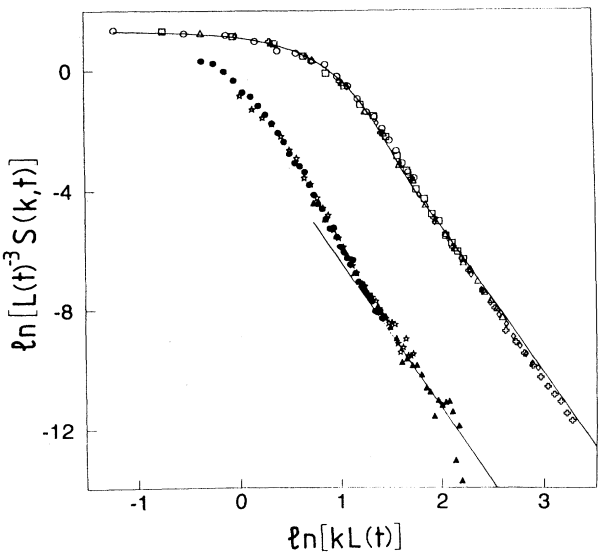

FIG. 3. Log-log plot for the scaled structure factor. Continuous curve: the O(2) theory; data points: simulation data from Ref. [9], rescaled as described in the caption to Fig. 2; the experimental data from Fig. 7 of Ref. [8] are shown on the left, arbitrarily positioned: they can be moved left-right and up-down. The straight line has slope -5. The simulation data contain an overall factor of $\frac{3}{4}$ that was inadvertently omitted in Ref. [9].

approximation given by (5) and (6), the dynamics (4) generates a finite string density, scaling as $L(t)^{-2}$, but a monopole density smaller than $L(t)^{-3}$. This is in accord with the experimental results of Yurke *et al.* [19], who also find that the monopole density decreases more rapidly than expected from naive scaling considerations.

To compute the structure factor $S(\mathbf{k},t)$, we Fourier-transformed various analytic fits to the Monte Carlo integration data for $C(12)$. Unfortunately, it was difficult to obtain results which were independent, to the accuracy we desired, of the fitting function used. However, the results were always very close to the structure factor for the O(2) theory [4] which, in real space, is scarcely distinguishable from the nematic liquid crystal (Fig. 2). The latter scaled structure factor is plotted, in log-log form, in Fig. 3, along with the simulation data from Ref. [9]. The agreement is good, even in the tail, despite the fact that a tail exponent of 5.3 was quoted for the simulation. Closer inspection of Fig. 3 provides an explanation: the data "overshoot" the eventual asymptotic line, and approach this line from above, giving a larger (i.e., more negative) effective exponent at smaller $kL(t)$. A similar feature is present in the theoretical curve.

The good agreement of simulation and theory is strong evidence for an asymptotic slope of -5. Also included in Fig. 3 are experimental data from Ref. [8]. We have not attempted a detailed comparison with theory: the experimental data can be moved left or right, and up or down, in the figure—the lack of structure in the data precludes any attempt at a precise fit. Moreover, it should be noted that both the present theory and the simulations of Ref. [9] exploit the simplifying equal-constant approximation [12], i.e., the assumption that the three terms in the Frank free energy, associated with splay, twist, and bend of the director, have equal amplitudes. It is not yet clear to what extent departures from this condition in real systems will affect experimentally determined scaling functions. The general form of the data, however, is in accordance with our theory and the simulation data. In particular, the overshoot feature is readily apparent: the gradient becomes less negative at larger $kL(t)$. A line of slope -5 has been included as a guide to the eye.

In conclusion, we have presented an approximate theory of phase-ordering dynamics in nematic liquid crystals. The results are in quantitative agreement with numerical simulations, and share many qualitative features with experimental data. The structure factor is predicted to exhibit a k^{-5} tail at large $kL(t)$.

We thank A. P. Y. Wong for sending us raw data from Ref. [8]. A.B., S.P., and A.S. thank the Physics Department of the University of Toronto, where this work was begun, and Rashmi Desai in particular, for his hospitality. R.B. thanks SERC (UK) for support; A.S. acknowledges support from Grant No. PB91-0090 of DGCyt (Spain); A.B. thanks A. J. McKane and M. A. Moore for discussions.

[1] T. J. Newman, A. J. Bray and M. A. Moore, Phys. Rev. B **42**, 4514 (1990); K. Humayun and A. J. Bray, J. Phys. A **23**, 5897 (1990).

[2] M. Mondello and N. Goldenfeld, Phys. Rev. A **42**, 5865 (1990); **45**, 657 (1992).

[3] H. Toyoki, Phys. Rev. A **42**, 911 (1990); J. Phys. Soc. Jpn. **60**, 1153 (1991); **60**, 1433 (1991).

[4] A. J. Bray and S. Puri, Phys. Rev. Lett. **67**, 2670 (1991); H. Toyoki, Phys. Rev. B **45**, 1965 (1992).

[5] Fong Liu and G. F. Mazenko, Phys. Rev. B **45**, 6989 (1992); A. J. Bray and K. Humayun, J. Phys. A **25**, 2191 (1992).

[6] A. Coniglio and M. Zannetti, Europhys. Lett. **10**, 575 (1989); A. J. Bray and K. Humayun, Phys. Rev. Lett. **68**, 1559 (1992).

[7] A. P. Y. Wong, P. Wiltzius, and B. Yurke, Phys. Rev. Lett. **68**, 3583 (1992).

[8] A. P. Y. Wong, P. Wiltzius, R. G. Larson, and B. Yurke (unpublished).

[9] R. E. Blundell and A. J. Bray, Phys. Rev. A **46**, 6154 (1992).

[10] A. J. Bray, Phys. Rev. E **47**, 228 (1993).

[11] G. Porod, in *Small-Angle X-ray Scattering*, edited by O. Glatter and O. Kratky (Academic, New York, 1982); P. Debye, H. R. Anderson, and H. Brumberger, J. Appl. Phys. **28**, 679 (1957); Y. Oono and S. Puri, Mod. Phys. Lett. B **2**, 861 (1988).

[12] P. G. de Gennes, *The Physics of Liquid Crystals* (Clarendon, Oxford, 1974).

[13] M. Kléman, *Points, Lines, and Walls, in Liquid Crystals, Magnetic Systems, and Various Ordered Media* (Wiley, New York, 1983).

[14] K. Binder and D. Stauffer, Phys. Rev. Lett. **33**, 1006 (1974); J. Marro, J. L. Lebowitz, and M. H. Kalos, *ibid.* **43**, 282 (1979); H. Furukawa, *ibid.* **43**, 136 (1979); Prog. Theor. Phys. **59**, 1072 (1978).

[15] A. J. Bray and K. Humayun, Phys. Rev. E **47**, 9 (1993).

[16] In fact, five of the ten integrals involved in our final expression can be evaluated analytically, and the remainder numerically, by changing variables to two (independent) eigenvalues, and three Euler angles, at each point. We have checked that this procedure gies the same results as our Monte Carlo integration.

[17] The growth law for $L(t)$ resulting from this fitting is close to the $t^{0.45}$ form obtained in Ref. [9], rather than $t^{1/2}$ as given by the theory. We cannot say whether this represents a real discrepancy, or indicates that the data are not yet in the asymptotic regime. Similar discrepancies occur for the O(2) theory (see Ref. [2]).

[18] R. E. Blundell and A. J. Bray (unpublished).

[19] B. Yurke, A. N. Pargellis, I. Chuang, and N. Turok, Physica B **178**, 56 (1992).